Published in final edited form as:
Environ Sci Technol. 2011 March 15; 45(6): 2227–2235. doi:10.1021/es102602s.

Comparison of the Johnson-Ettinger Vapor Intrusion Screening Model Predictions with Full Three-Dimensional Model Results

Yijun Yao, **Rui Shen**, **Kelly G. Pennell**[#], and **Eric M. Suuberg**[*]
School of Engineering, Brown University, Providence RI02912

Abstract

The Johnson-Ettinger vapor intrusion model (J-E model) is the most widely used screening tool for evaluating vapor intrusion potential because of its simplicity and convenience of use. Since its introduction about twenty years ago, the J-E model has become a cornerstone in guidance related to the potential for significant vapor intrusion-related exposures. A few papers have been published that claim it is a conservative predictor of exposure, but there has not been a systematic comparison in the open literature of the J-E model predictions with the results of more complete full three-dimensional descriptions of the phenomenon. In this paper, predictions from a three-dimensional model of vapor intrusion, based upon finite element calculations of homogeneous soil scenarios, are directly compared with the results of the J-E model. These results suggest conditions under which the J-E model predictions might be quite reasonable, but others in which the predictions are low as well as high. Some small modifications to the J-E model are also suggested that can bring its predictions into excellent agreement with those of the much more elaborate 3-D models, in some specific cases of homogeneous soils. Finally, both models were compared with actual field data.

Introduction

The vapor intrusion (VI) problem has been the focus of a series of modeling studies, starting with a focus on radon (1–2) and more recently concerned with contaminants of anthropogenic origin (3–19). Several numerical models have been developed and proven to be useful tools in understanding the phenomenon, since the first identification of the probable VI pathway into a building in 1987(1).

With improvement over time in understanding of VI processes, different kinds of models have been developed to assess the potential for indoor air quality problems. These models range from simple screening, one-dimensional (1-D) models (e.g. Johnson and Ettinger model) (3) to full three-dimensional (3-D) fluid flow models (7, 9, 15–17). Among the former class of models, the Johnson-Ettinger (J-E) model (3) is the most widely used in the US. This model was proposed as a screening tool in the preliminary 2002 US EPA Vapor Intrusion Guidance (5). Prior and subsequent to issuance of that guidance, the J-E model has come under considerable scrutiny, and even some suggestion from within EPA that the screening tool should be reevaluated (11). Several useful articles have been written to clarify proper application of the J-E model as a screening tool for identifying the potential for VI problems, rather than as a quantitative predictive model (4, 7, 9), and it has been judged to be conservative in many cases (6), though not conservative enough in others (10). There are

[*]Corresponding author phone: (401) 863-1420; Eric_Suuberg@Brown.EDU. [#]Current address: Department of Civil & Environmental Engineering University of Massachusetts-Dartmouth, Dartmouth MA02747; kpennell@umassd.edu.

Supporting Information Available
Tabulated results for Figure 3 and Table 4 are available free of charge via the Internet at http://pubs.acs.org.

numerous other screening tools in use worldwide and these have also been recently reviewed (18–19). Again, the other simple screening models tended to over-predict measured concentrations, but the J-E model was one of two that was judged to provide closest agreement with actual measurements (18).

It is also important to recognize that what is commonly referred to as the J-E model is actually the U.S. EPA spreadsheet implementation of what was originally proposed by Johnson and Ettinger, as noted by Johnson in 2005 (4, 8). It is this EPA version of the model that was examined in this paper, since this is the version in widest use. Even then, there are multiple versions of this model offered on the EPA website. The version used to obtain the results presented here was the soil vapor screening model (SG-ADV-Feb04).

Two basic assumptions of the J-E model are also examined in this paper: that of diffusion dominated transport in the domain and the other, mass conservation from a source to the enclosed space built atop that source.

The Models

The Full Three-Dimensional F inite Element Model of Vapor Intrusion

The full 3-D model examined here is essentially that presented earlier by this group. (15–17). The case of interest here is the earlier discussed steady-state “base case”, i.e., a single structure built atop an otherwise flat, open field, underlain by a homogeneous soil that stretches from the ground surface to a water table serving as an infinite source of the contaminant of interest. The important influence of soil layering, soil inhomogeneities and surface capping were earlier discussed (15–17), but these are not considered here. The assumed domain size here was smaller than that in earlier base cases, but this is of no consequence to the results. Also, the earlier “Characteristic Entrance Region (CER)” approximation to crack geometry was not needed here (15–17), and had no significant impact on results.

The modeled situation consists of a single square 10m × 10 m footprint structure built on otherwise open (uncapped) field of 24 m × 24 m (see Figure 1). This domain size is sufficiently large such that the boundaries do not substantially affect the solution within the domain. The structure has either a basement foundation or is built on a slab. For simplicity, the results are based on the commonly assumed 0.005 m wide perimeter crack scenario. The crack is assumed to run along the entire edge of the foundation or slab, and the influences of different types of foundation openings are the focus of ongoing research by the authors.

The key working equations are summarized in Table 1. Incompressible soil gas flow is assumed, as is typical. All contaminant vapor originates from the groundwater surface, and there are no contaminant sources within the soil itself. The pressure driving force for soil gas advection arises from the “chimney effect” within the structure itself, transmitted to the soil through the foundation perimeter crack, which itself is also the main pathway for contaminant vapor entry into the building.

Fundamentally, the equations in Table 1 are present in the J-E model as well, except that they represent one-dimensional, as opposed to three-dimensional processes (see below). All inputs to the three-dimensional model were the same as used in the J-E model, except as noted below.

Since all scenarios modeled in this paper involve the illustrated symmetrical situation, simulation of only a quarter of the Figure 1 (a) domain fully defines the solution, as illustrated in Figure 1b. (Contaminant mass entry rates given below are for the whole domain). Planes of symmetry, the groundwater surface and the foundation (except for the

crack) are all no-flux boundaries, whereas the open ground surface is taken to be at atmospheric reference pressure and is a sink of zero contaminant concentration.

Table 2 gives the key input parameters explored in this study. Though permeability and diffusivity are both related to the porosity of the soil (17), small variations in diffusivity do not have a significant impact on solution. For purposes of presenting a consistent comparison, a constant effective soil porosity and diffusivity were assumed here, and again, small changes in these values had little effect on the conclusions. It should also be noted that while the simulations were carried out for trichloroethylene (TCE) in the case of the J-E model, the choice of contaminant is largely unimportant because most volatile organic compounds (VOCs) of concern have similar diffusivity values.

The Johnson-Ettinger model

The Johnson-Ettinger model considered here is mainly based on two (steady state) working equations. The first expresses the fact that the contaminant released at the source must enter the crack (equation (5)), and the second (equation (6)) shows that indoor air concentration is determined by building air exchange

$$\frac{D_{eff} * A_B}{L_T}(c_{source} - c_{ck}) = Q_{ck} * \frac{exp\left(\frac{Q_{ck} d_{ck}}{A_{ck} D^{ck}}\right) c_{ck} - c_{indoor}}{exp\left(\frac{Q_{ck} d_{ck}}{A_{ck} D^{ck}}\right) - 1} \quad (5)$$

$$Q_{ck} * \frac{exp\left(\frac{Q_{ck} d_{ck}}{A_{ck} D^{ck}}\right) c_{ck} - c_{indoor}}{exp\left(\frac{Q_{ck} d_{ck}}{A_{ck} D^{ck}}\right) - 1} = Q_{building} * c_{indoor} \quad (6)$$

Where c_{source} is the soil vapor concentration of the source, L_T is the distance from source to the bottom of the foundation, A_B is the surface area of enclosed space below grade and D^{ck} is the effective diffusivity of air in the crack (other symbols defined as in Table 1). The results of the J-E model are often presented in terms of the indoor air concentration attenuation factor (α), which may be solved for from the above two equations:

$$\alpha = \frac{c_{indoor}}{c_{source}} = \frac{\frac{D_{eff} * A_B}{Q_{building} L_T} exp\left(\frac{Q_{ck} d_{ck}}{A_{ck} D^{ck}}\right)}{exp\left(\frac{Q_{ck} d_{ck}}{A_{ck} D^{ck}}\right) + \frac{D_{eff} * A_B}{Q_{ck} L_T}\left(exp\left(\frac{Q_{ck} d_{ck}}{A_{ck} D^{ck}}\right) - 1\right) + \frac{D_{eff} * A_B}{Q_{building} L_T}} \quad (7)$$

Estimates of soil gas entry rate

Any pressure-driven soil gas flow into a foundation crack can enhance contaminant entry rate over that which would exist due to pure diffusion through the crack, through advective conveying of contaminant into the building. This aspect of the VI phenomenon is already well understood and generally accepted in current models. In the J-E model of USEPA spreedsheet, the estimate of this flow, Q_{ck}, is based upon the work of Nazaroff and his colleagues (2), and is embodied in a simple approximation based on flow into a buried porous pipe-like structure. Johnson has suggested that the Johnson and Ettinger (1991) equation and the USEPA spreadsheets be reformulated so that the ratio of $Q_{ck}/Q_{building}$ would be used to replace Q_{ck} from Nazaroff's equation (8). This has not been done here, in keeping with what is presently used.

The equation developed by Nazaroff for this soil gas volumetric advection into a buried pipe is:

$$Q_{ck\_Na} = \frac{2\pi k \Delta p L_{ck}}{\mu_g \, ln(2d_f / r_p)} \quad (8)$$

In which L_{ck} is the length of a hypothetical buried pipe, d_f is the depth of the pipe below the soil surface and r_p is the radius of pipe, and other symbols as already defined.

In the J-E model, a perimeter crack is approximated by a form equivalent to the buried pipe. The soil gas flow rate is approximated by a transformed equation

$$Q_{ck\_JE} = \frac{2\pi k \Delta p L_{ck}}{\mu_g \, ln(2d_f / w_{ck})} \quad (9)$$

Where r_p is replaced by crack width.

For a perimeter crack, a crack velocity may be calculated from Q_{ck}:

$$\bar{v}_{ck} = \frac{Q_{ck}}{A_{ck}} \quad (10)$$

$$A_{ck} = L_{ck} W_{ck} \quad (11)$$

The average velocity $\bar{v}_{ck}$ can be used to define a non-dimensional characteristic velocity U,

$$\mathrm{U} \equiv \left(\frac{\bar{v}_{ck}}{\bar{v}_{cko}}\right)\left(\frac{k_o}{k}\right)\left(\frac{\Delta p_o}{\Delta p}\right) \quad (12)$$

In which k is the soil permeability and k_o is a base case permeability of 10^{-11} m^2, Δp is the pressure differential between the crack entrance and atmosphere, and Δp_o is the base case pressure differential of −5 Pa. d_{fo} is the base case foundation depth of 2 m, this leads to a standard reference velocity of $\bar{v}_{cko} = 5.04 \times 10^{-4}$ m/s, calculated using the J-E model. The above non-dimensionalization recognizes the linearity of flow velocities with respect to soil permeability and pressure driving force, and chooses a reference velocity characteristic of typical parameter choices.

Figure 2 (a) presents the results of the full 3-D simulations results for advective soil gas entry rates into the structure, and are nondimensionalized using equation (9). In this instance, the calculation involved $k = ko = 10^{-11}\ m^2$ and $\Delta p = \Delta p_o = -5\ Pa$. If the 3-D model and the J-E model were in agreement, U would equal 1 for the $d_f = d_{fo} = 2$ m deep basement scenario. The slab on grade condition is represented by a foundation depth of 0.1 m, and other depths are also shown, corresponding to possible crawl-space or basement conditions. It is apparent that the J-E model actually provides a very good approximation to the more detailed solution provided by solving the full fluid mechanics equation, but it typically overpredicts the entry rate (the reference velocity in (12) is too high, which is why the detailed simulation results are all seen to give U less than unity). The apparent overprediction of entry velocity is seen to be near a factor of two in most cases, though a bit less in the case of the slab. The source depth is seen to be of no consequence. Similar results were obtained for different permeabilities.

This means that the estimate of the advective entry rate assumed in the case of the J-E model can be slightly improved. One step of improvement involves assuming that only half of the hypothetical buried pipe surface is available for receiving flow from the soil, which recognizes the top half of the pipe cannot receive flow because it is immediately adjacent to the building floor (2). The other small improvement is to relate the crack half-width to pipe radius, which is in better agreement with Naarooff' original approximation (Equation 8). The results of these modifications are shown in equations (13) and (14):

$$Q_{ck\_MNa} = \frac{\pi k \Delta p L_{ck}}{\mu_g \, ln(4d_f / w_{ck})} \quad (13)$$

$$U_{MNa} = \left(\frac{\bar{v}_{ck}}{\bar{v}_{cko}}\right)\left(\frac{k_o}{k}\right)\left(\frac{\Delta p_o}{\Delta p}\right) = \frac{ln(2d_{fo}/w_{ck})}{2\, ln(4d_f/w_{ck})} \quad (14)$$

The results of these modifications are shown in Figure 2 (b), in which the result of the J-E model estimate is compared with the detailed 3-D simulation results and the modified Nazaroff approximation, using equations (13) and (14). Similar agreement is achieved with different values of k (10^{-10}–10^{-14} m^2) and Δp (0–20 Pa).

There are few specified experimental results using tracer tools, which offer insight into how well such models can predict gas entry rates. A relevant selection is given in Table 3 (6). In some cases, the modified approach provided the expected better agreement, and in others not. The bottom line is that overall the modified equation does seem to fit fairly well.

Comparison of the full 3-D Simulation with Predictions of the Johnson-Ettinger Model

The results of the attenuation factor predictions from the J-E model can be compared with the results of the full 3-D simulations. This is first done in Figure 3 (a) for the J-E model, as implemented by EPA. Figure 3 (a) shows the comparison for different soil permeabilities and source depths. It may be quickly seen in the case of unusually high permeability soils (K =10^{-10} m^2) that the J-E model predictions are generally low, as compared with the full 3-D simulation. In the more typical soil permeability range (k = 10^{-11} to 10^{-12} m^2), the J-E model predictions are seen to be conservative as compared to the full 3-D simulation predictions, which was also pointed out by others (6). With low permeability, clay-like soils (10^{-13}–10^{-14} m^2), the J-E results generally under-predict, as compared with a full 3-D simulation.

Figure 3 (b) shows the same sorts of predictions as in Figure 3 (a), but in this case, for a simulated slab-on-grade scenario. The same general trend is seen with the highest permeability soil as in the 2 m deep foundation case, but in this case, the J-E model predictions are generally conservative even for lower permeability soils. It is worth noting that in virtually all cases, the J-E model predictions are within an order of magnitude of the more detailed 3-D simulation results. This is certainly affirmation of the value of the simple J-E screening tool in geologically simple scenarios.

It has already been noted that the J-E model uses a soil gas entry rate that is a bit high compared with full 3-D simulation. It is of interest to see the influence of employing the presumably more accurate estimate of that velocity, such as provided by a detailed 3-D calculation of that velocity. In addition, the effective diffusivity in the crack used in the JE model is often taken to be that in the soil, whereas the higher molecular diffusivity of

contaminant in air has been used to model the crack in our full 3-D simulations, (and this assumption was also used in Johnson's later research (7,9)). To explore the influence of these differences, comparisons were made between the full 3-D simulations and the J-E model modified in only these two ways. Results corresponding to those in Figure 3 (a) and (b) are provided in Figure 3 (c) and (d); the results for the 3-D simulations are the same as in Figure 3 (a) and (b), since it was only the J-E model results that changed.

In Figure 3 (c), the predictions of indoor air contaminant concentration slightly decreased for the higher soil permeabilities, as would be expected as a result of a lower soil gas entry flow rates. On the other hand, the revised J-E model predictions for the lower soil gas permeabilities greatly increased, by virtue of the higher diffusivity assumed in the crack (since the advective contribution to contaminant entry is minimal, under those conditions). In Figure 3 (d), for the slab on grade, the revised J-E model results tend to cluster in a narrow band, and are often quite conservative, relative to the full 3-D simulation results (again, except for the unusually high permeability soil, in which the revised J-E model again under-predicts relative to the full simulation). Thus the importance of the crack diffusivity assumption is illustrated.

According to the 3-D model, the subslab or crack concentration is mainly determined by the geometry of the domain and not by soil permeability or diffusivity. In high permeability cases, where convection is determining the contaminant mass flow through the crack, and the solution is thus not sensitive to the diffusivity of the contaminant in the soil. This is not true for the J-E model, because of its requirement of mass balance between contaminant transport in the soil and its mass flow into the house. Thus the soil diffusivity also makes a difference in the J-E model prediction, just as did the crack diffusivity.

Figure 4 shows the J-E model predicted variation in α with contaminant soil diffusivity. In general, α is linear in soil diffusivity, with other conditions unchanged. For 3-D simulation, α is not sensitive to soil diffusivity for high permeability because it is advection that then dominates contaminant entry rate. Even for low permeability, α is much less sensitive to soil diffusivity than that in the J-E model. This is an important difference between the model predictions.

Mass Conservation Considerations

The original J-E model was based on two important assumptions. The first is that diffusion dominates contaminant transport through the soil (and this is what determines soil gas contaminant concentration profiles). This has been affirmed by the more detailed simulations as well (15–17). Thus, the role of advection in establishing the contaminant soil gas profile is actually quite minimal. Where advection plays a role is in pulling contaminant into the structure from a diffusion-determined zone of high concentration beneath the structure.

The second assumption in the J-E model development was that of mass conservation in contaminant transport. In the J-E model, the surface area of the enclosed space in contact with soil was used as the effective source area, which arises from the need to maintain a 1-D modeling approach, in which the contaminant only moves upward from a source beneath the structure, and cannot be lost by diffusion in an orthogonal direction (nor augmented by inward diffusion from outside of the footprint). This is clearly a significant restriction, and it is worthwhile examining its consequences.

Figure 5 (a) shows, from the detailed 3-D simulations, the flux of contaminant from a source beneath the building, J, as a function of soil permeability. This quantity J is simply the mass

flux over the whole domain, normalized by the theoretical diffusion flux between a source at c_{source} and a sink at zero, using the depth of source as the diffusion path length:

$$J=\frac{M_{released}d_{source}}{A_{source}D_{eff}c_{source}} \quad (15)$$

Where $M_{released}$ is the contaminant mass flow rate from the source and A_{source} is the area of the source, both of which were from 3-D simulation.

Not surprisingly, consistent with a diffusion-dominated release of contaminant from the source, the value of J is very near unity for all cases. The presence of the structure on the domain does not change this fact. This conclusion is independent of soil permeability, except when the permeability gets very high, and even then, the influence on contaminant release rate is quite modest. (The value of J goes up to only about 1.4; i.e. a 40% increase)

Figure 5 (b) shows a “MAss Conservation”, defined as:

$$R_f=\frac{M_{ck}}{M_{f-released}} \quad (16)$$

Where M_{ck} is the calculated contaminant entry rate into the crack and where $M_{f-released}$ is the release rate of the contaminant from the source directly beneath the building footprint. The release rate from directly beneath the foundation may be calculated from

$$M_{f-released}=M_{released}\frac{A_{foundation}}{A_{source}} \quad (17)$$

For a 10 m × 10 m footprint foundation, $A_{foundation}$ =100 m^2, where necessary account is taken for the quarter domain calculation. It is important to note that Figure 5 is for the model parameters specified in this paper; i.e. pressure difference and effective diffusivity.

It is apparent that only a small fraction of the mass released beneath the structure might actually enter the structure. This in effect shows the “violation” of the situation that is involved in the J-E modeling approximation. In the case of a soil permeability of 10^{-11} m^2, the approximation is actually quite good (especially for the 2 m depth foundation case), but for higher permeability, contaminant entry can actually be enhanced by soil gas drawn in from outside of the building footprint. In the case of low permeability soils, much of the contaminant released beneath the building is lost to diffusion away from the building. This is seen to be relatively insensitive to the source depth, explaining why the J-E model is relatively conservative as compared with the detailed 3-D simulation.

Since Figure 5 (b) shows that the mass conservation ratio is independent of source depth, these results can be averaged irrespective of depth to provide one further “correction” to the one-dimensional J-E model. In this approach, the left hand side of equation (5) may be modified using the value of R_f from this figure to correct for the fraction of contaminant released beneath the building that actually enters the building. This value is independent of source concentration or depth, but does depend upon the value of D_{eff} and, of course, k. The resulting corrected equation for α is:

$$\alpha = \frac{c_{indoor}}{c_{source}} = \frac{\frac{D_{eff} * A_B}{Q_{building} L_T} exp\left(\frac{Q_{ck} d_{ck}}{A_{ck} D^{ck}}\right)}{\frac{1}{R_f} exp\left(\frac{Q_{ck} d_{ck}}{A_{ck} D^{ck}}\right) + \frac{D_{eff} * A_B}{Q_{ck} L_T}\left(exp\left(\frac{Q_{ck} d_{ck}}{A_{ck} D^{ck}}\right) - 1\right) + \frac{D_{eff} * A_B}{Q_{building} L_T}} \quad (18)$$

Application of this correction along with the previously described modifications to the JE model, result in the predictions shown in Figure 3 (e) and (f). In some respects, it may be argued that this correction is circular in nature; that is, the J-E model is being forced to fit the 3-D simulation results by applying those same results as a correction. On the other hand, note that the mass conservation correction is really, to an excellent approximation, only a function of soil permeability in the specified cases. It simply reflects the interplay between diffusion and advection, which needs to be accounted for in many soils, which is not reflected in the pure 1-D formulation.

Model results and field data

The work by Hers et al. (5) has already established that the predictions of the J-E model are in reasonable agreement with a great deal of field data, if perhaps a bit on the conservative side. This reasonable agreement, when considered in the context of the generally fair to good agreement between the J-E model and the 3-D model considered here, already helps establish that the latter is providing reasonable results. Recognizing, too, that the 3-D model is built upon a structure suggested by the earlier radon modeling work (and its validation), the latter comes as little surprise.

The main purpose of this study was not to provide a validation of any particular VI modeling approach, but to provide a comparison of the results from the J-E approach to a full 3-D model, for the same set of input parameters. Again, the sensitivity of the respective models to the input parameters has been recognized and noted in previously published articles (5, 14–15), but the choice to use the same parameter sets here makes the comparison as consistent as possible. The comparison ranges from good to fair, and this is the key conclusion of this paper.

This might still leave open a question as to whether it can be shown that the 3-D simulation by itself offers reasonable predictions, and this led to offering the very basic comparison in Table 4 of the full 3-D model predictions to some results obtained from an actual PCE contaminated site located in New England. The details of this site (and consultant-provided field data) are provided in the supplemental material.

Again, it is recognized that this does not yet by any means represent a full validation of the 3-D model, but it is a first step in this direction and other results are being obtained by us from this same site. What are shown are the indoor and subslab concentrations of PCE (here, the subslab value is taken to be the value at the inlet to an assumed perimeter crack).

In general, the 3-D simulations and EPA version of the J-E model both provide reasonable estimates of indoor air and subslab concentrations. There were no indoor depressurization nor air exchange data to guide the modeling work, so a typical air exchange rate of 0.45/hr was assumed, and two different extents of indoor depressurization were assumed (−5 and −20 Pa), as shown. The ranges shown are for the upper and lower limits of concentrations, shown in Table 5 of the supplemental materials, but briefly, the measured basement concentration of PCE was 163 $\mu g/m^3$, while the subslab concentrations varied from 16,400 to 21,600 $\mu g/m^3$ and the groundwater concentration of PCE ranged from 198–261 $\mu g/L$. Applying the corrections discussed above to the J−E model, the agreement between that model and measurements is even better.

Based on the research in the work, it is seen that the J-E model (as implemented by EPA) provides a good approximation to the results of a 3-D simulation, generally to within an order of magnitude in indoor air attenuation factor. However, it is possible to improve the theoretical basis of the J-E model approximation even further by making small changes to the estimate of soil gas entry rate and recognizing the restriction that an assumption of contaminant mass conservation places upon a 1-D model such as J-E. Also the difference in the role that advection and diffusion play in establishing contaminant entry rates has been highlighted.

Supplementary Material

Refer to Web version on PubMed Central for supplementary material.

Literature Cited

1. Nazaroff WW, Lewls SR, Doyle SM, Moed BA, Nero AV. Experiments on pollutant transport from soil into residential basements by pressure-driven airflow. Environ Sci Technol. 1987; 21:459–466. [PubMed: 22296133]
2. Nazaroff WW. Predicting the rate of ^{222}Rn Entry from soil into basement of a dwelling due to pressure-driven air flow. Radiation Protection Dosimetry. 1988; 24:199–202.
3. Johnson PC, Ettinger RA. Heuristic model for predicting the intrusion rate of contaminant vapors into buildings. Environ Sci Technol. 1991; 25:1445–1452.
4. Johnson PC. Identification of critical parameters for the Johnson and Ettinger 1991 vapor intrusion model. Ground WaterMonit Rem. 2005 winter;25(1):63–78.
5. U.S. Environmental Protection Agency. OSWER draft guidance for evaluating the vapor intrusion to indoor air pathway from groundwater and soils. EPA; Washington, DC: 2002.
6. Hers I, Zapf-Gilje R, Johnson PC, Li L. Evaluation of the Johnson and Ettinger model for the prediction of indoor air quality. Ground Water Monitoring & Remediation. 2003; 23(1):62–76.
7. Abreu LD, Johnson PC. Effect of vapor source-building separation and building construction on soil vapor intrusion as studied with a three-dimensional numerical model. Environ Sci Technol. 2005; 39:4550–4561. [PubMed: 16047792]
8. Johnson PC. Identification of application-specific critical inputs for the 1991 Johnson and Ettinger vapor intrusion algorithm. Ground Water Monitoring and Remediation. 2005; 25(1):63–78.
9. Abreu LD, Johnson PC. Simulating the effect of aerobic biodegradation on soil vapor intrusion into buildings: influence of degradation rate, source concentration, and depth. Environ Sci Technol. 2006; 40:2304–2315. [PubMed: 16646467]
10. Tillman FD, Weaver JW. Uncertainty from synergistic effects of multiple parameters in the Johnson and Ettinger (1991) vapor intrusion model. Atmospheric Environment. 2006; 40(22): 4098–4112.
11. Schuver, H. Role of modeling & general status of revisions to EPA's 2002 vapor intrusion guidance. Updated J&E Model Spreadsheets Workshop AEHS Spring 2006 Meeting; March 16, 2006;
12. Devall GE. Indoor vapor intrusion with oxygen-limited biodegradation for a subsurface gasoline source. Environ Sci Technol. 2007; 41:3241–3248. [PubMed: 17539532]
13. Mills WB, Liu S, Rigby MC, Brenner D. Time-variable simulation of soil vapor intrusion into a building with a combined crawl space and basement. Environ Sci Technol. 2007; 41:4993–5001. [PubMed: 17711214]
14. Patterson BM, Davis GB. Quantification of vapor intrusion pathways into a slab-on-ground building under varying Environmental Conditions. Environ Sci Technol. 2009; 43:650–656. [PubMed: 19244997]
15. Pennell KG, Bozkurt O, Suuberg EM. Development and application of a three-dimensional finite element vapor intrusion model. J Air & Waste Manage Assoc. 2009; 59:447–460.

16. Bozkurt O, Pennell KG, Suuberg EM. Simulation of the vapor intrusion process for nonhomogenous soils using a three-dimensional numerical model. Ground Water Monitoring & Remediation. 2009; 29:92–104. [PubMed: 20664816]

17. Bozkurt, O. PhD Dissertation. Brown University; Providence, RI: 2009. Investigation of Vapor Intrusion Scenarios using a 3D numerical model.

18. Provoost J, Reijnders L, Swartjes F, Bronders J, Seuntjens P, Lijzen J. Accuracy of seven vapour intrusion algorithms for VOC in groundwater. J Soils Sediments. 2009; 9(1):62–73.

19. Provoost J, Bosman A, Reijinder L, Bronders J, Touchant K, Swartjes F. Vapour intrusion from the vadose zone-----seven algorithms compared. J Soils Sediments. 2010; 10:473–483.

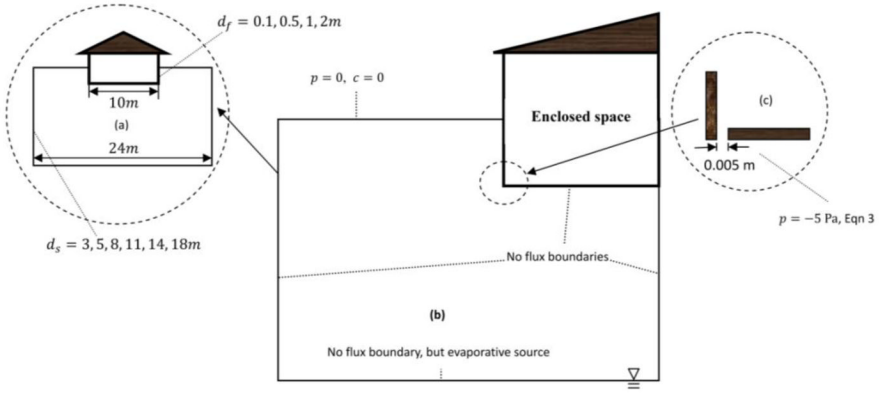

Figure 1.
Cross sectional view of (a) full domain of interest (b) boundary conditions of modeled quarter domain (c) details of modeled perimeter crack

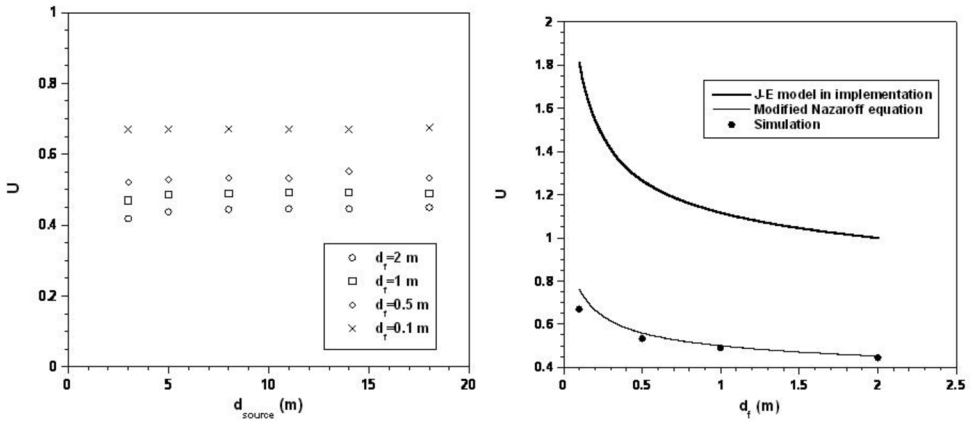

(a) (b)

Figure 2.

(a) The influence of foundation depth and depth of source on the soil gas entry flow through a perimeter crack based on 3-D simulation. (b) Estimates of the soil gas flow through the crack using different calculational methods.

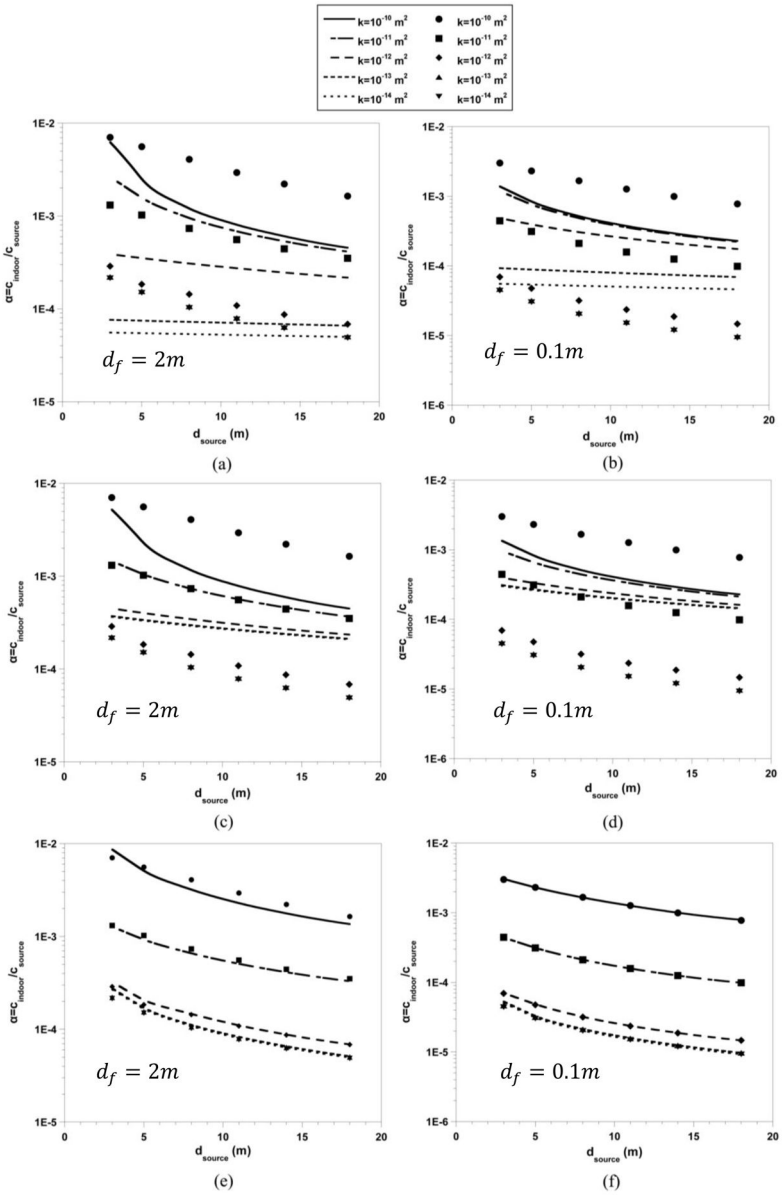

Figure 3.

The comparison of the EPA implementation of the J-E model (curves) with the full 3-D simulation (points) for a 2m depth foundation (a) and a 0.1m depth foundation (b); the comparison of the revised J-E model (flow and diffusivity corrections) results with those of the full 3-D simulation, for a 2 m depth foundation (c) and a 0.1m depth foundation (d); The comparison of the revised J-E model (curves, which include flow, diffusivity and mass conservation corrections) on indoor air concentration attenuation factor with detailed simulation results (points) for a 2m deep foundation (e) and a 0.1m depth foundation (f).

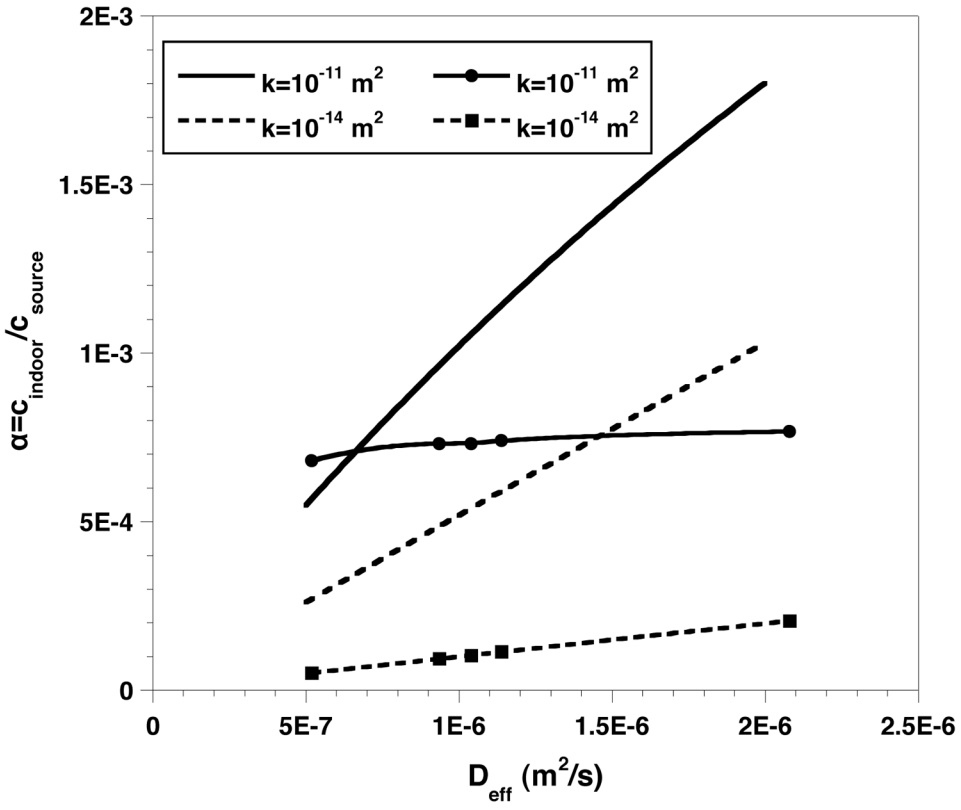

Figure 4.

The relationship between indoor air concentration attenuation factor and effective diffusivity for a source at 8m bgs for the J-E model. (Here, the modified Q_{ck} and D^{crack} corresponding to gas-phase diffusivity have been used; Lines are from the J-E model, and points are from 3-D simulation).

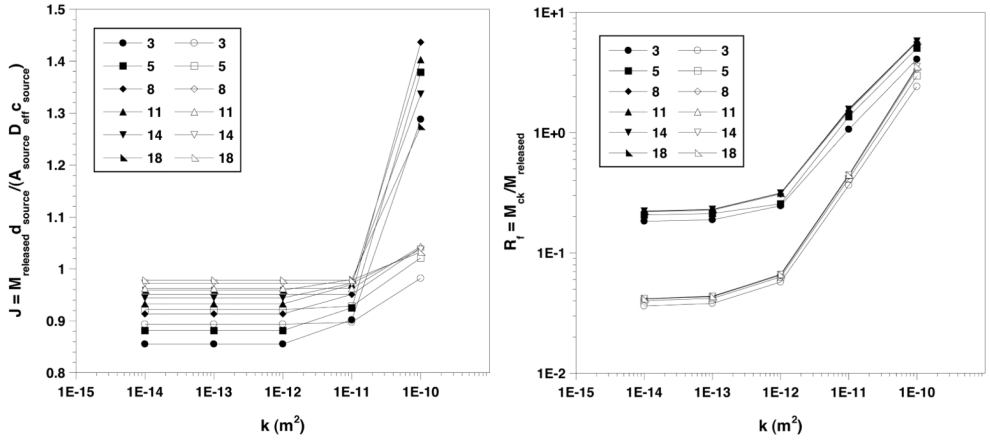

(a) (b)

Figure 5.

(a) The influence of soil permeability on contaminant release rate from the source based on 3-D simulation for 2m (solid points) and 0.1m (open points) depth foundation. (b) The influence of soil permeability on mass conservation ratio from 3-D simulation for 2m (solid points) and 0.1m (open points) depth foundation. The values in the legends refer to source depth (m).

Table 1

Summary of model equations for steady state simulation (15).

Equation 1: Soil gas continuity $q=-\frac{k\rho_g}{\mu_g}\nabla\varphi$ $\varphi=gz+\int_{p_0}^{p}\frac{\nabla p}{\rho_g}$	Where: q = Soil gas velocity (L/t) k = Intrinsic permeability (L^2) ρ_g = Density of soil gas (M/L^3) μ_g = Dynamic viscosity of soil gas (M/L/t) g = Gravitational acceleration (L/t^2) z = Elevation (L) p = Pressure of soil gas ($M/L/t^2$)
Equation 2: Chemical transport $J_T=qc-D_{eff}\nabla c$ $D_{eff}=D^g\frac{\varphi_g^{\frac{10}{3}}}{\varphi_T^{\,2}}+\frac{D^w}{H}\frac{\varphi_w^{\frac{10}{3}}}{\varphi_T^{\,2}}\approx D^g\frac{\varphi_g^{\frac{10}{3}}}{\varphi_T^{\,2}}$	Where: J_T = Bulk mass flux of chemical ($M/L^2/T$) D_{eff} = Effective diffusivity coefficient of chemical in soil gas phase (L^2/T) D^g = Molecular diffusion coefficient for chemical in gas (L^2/T) D^w = Molecular diffusion coefficient for chemical in water (L^2/T) c = Concentration of chemical in soil gas (M/L^3) H = Air:water partition (Henry's) coefficient (L^3_{air}/L^3_{water}) φ_g = Porosity filled by gas (L^3_{air}/L^3_{soil}) φ_w = Porosity filled by water(L^3_{water}/L^3_{soil}) φ_T = Total porosity (L^3_{pores}/L^3_{soil})
Equation 3: Chemical mass flux through the crack $J_{ck}=q_{ck}\frac{exp\left(\frac{q_{ck}d_{ck}}{D^g}\right)c_{ck}-c_{indoor}}{exp\left(\frac{q_{ck}d_{ck}}{D^g}\right)-1}$ $\approx\frac{q_{ck}exp\left(\frac{q_{ck}d_{ck}}{D^g}\right)c_{ck}}{exp\left(\frac{q_{ck}d_{ck}}{D^g}\right)-1}\ (q_{ck}\neq 0)$	Where: J_{ck} = Mass flux of chemical ($M/L^2/T$) q_{ck} = Soil gas velocity at the crack (L/T), from solution of Darcy's Law. d_{ck} = Thickness of the crack (L) c_{ck} = Concentration of chemical at the crack (M/L^3)
Equation 4: Indoor air concentration: $c_{indoor}=\frac{M_{ck}}{Q_{ck}+V_bA_e}\approx\frac{M_{ck}}{V_bA_e}$ $=\frac{M_{ck}}{Q_{building}}$	Where: c_{indoor} = Concentration of chemical in the indoor air (M/L^3) M_{ck} = Mass flow rate of chemical through the crack (M/T) V_b = Volume of enclosed space (L^3) A_e = Air exchange rate of building (T^{-1}) Q_{ck} = Volumetric flow rate through the crack (L^3/T) $Q_{building}$ = Building ventilation rate (L^3/T)

Table 2

Input parameters used in 3-D simulation (unless otherwise noted in the figures and table)

Building/foundation parameters
Foundation foot print length: 10 m, width: 10 m
Depth of foundation (d_f): 0.1 and 2 m
Crack/foundation slab thickness (d_{ck}): 0.152 m
Crack width (w_{ck}): 0.005 m
Crack area (A_{ck}): 0.199 m^2
Volume of intruded area (V_b): 3.66×10^2 m^3
Air exchange rate in intruded volume (A_e) 0.25 hr^{-1}
Depth to groundwater/source (d_{source}) 3, 5, 8, 11, 14, 18 m bgs
3-D Finite Element Analysis Parameters
Size of the grid elements: 0.001 m – 1 m
Number of elements: 200k – 600k
Contaminant vapor source properties
Contaminant: TCE
Diffusivity of TCE in crack (D^{ck}): 7.4×10^{-6} m^2/s
Diffusivity of TCE in air (D^a): 7.4×10^{-6} m^2/s
Effective diffusivity of TCE in soil (D_{eff}): 1.04×10^{-6} m^2/s
Soil gas flow properties
Viscosity of air/soil gas (μ_g): 1.8648×10^{-5} kg/m/s
Density of air/soil gas (ρ_g): 1.1614 kg/m^3
Soil permeability (k): 10^{-10}, 10^{-11}, 10^{-12}, 10^{-13} and 10^{-14} m^2
Total soil porosity (φ_t): 0.35
Soil porosity filled with gas (φ_g): 0.296

TABLE 3

Comparison of measured and model-predicted soil gas flow rates into building (6)

Site	Foundation type	Measured (L/min)	Q_{ck_JE} (L/min)	Q_{ck_MNa} (L/min)
	Slab-on-grade	2.7	29	13.2
Chatterton Site (Hers et al. 2000)	Slab-on-grade	4.2	9.6	4.4
	Slab-on-grade	2.9	8.2	3.8
Alameda Site (Fischer et al. 1996)	Slab-on-grade	1.4	2.4	1.1
Spokane Valley Houses (Revzan et al. 1991)	Basement	102	110	51.0

Table 4

Comparison of field data (R_f = 0.8 for Δp = −5 Pa and R_f = 2.4 for Δp = −20 Pa)

	Δ*p* (Pa)	**Measured**	**3-D simulation**	**EPA J-E model**	**Modified J-E model with R_f from Figure 5(b)**
c_{ck}/c_{source}	−5	0.06 – 0.11[a]	0.46	0.34	0.34
	−20		0.36	0.11	0.28
$\alpha = c_{indoor}/c_{source}$	−5	6.2e-4 – 8.2e-4[b]	2.1e-04	3.3e-4	1.9e-4
	−20		6.4e-04	4.4e-4	6.2e-4

[a] range of values based upon actual measured groundwater source and subslab soil vapor concentration values

[b] range of values based upon actual measured groundwater source and indoor air concentration values